TITLE

Transport Dynamics Across Prebiotic Hydrothermal Mineral Barriers: Comparison with Contemporary Proton Motive Pathways

AUTHORS

Thiago Altair[1,2], Douglas Galante[3], Hamilton Varela[2], Yannick De Decker[4], Reuben Hudson[1,5]

AUTHOR ADDRESS. [1]College of the Atlantic, Bar Harbor, ME, 04609, USA, [2] São Carlos Institute of Chemistry, University of São Paulo, São Carlos 13560-970, Brazil, [3] Institute of Geosciences, University of Sao Paulo, Sao Paulo 05508-080 Brazil, [4]Center for Nonlinear Phenomena and Complex Systems (CENOLI), Université libre de Bruxelles (ULB), Campus Plaine, C.P. 231, B-1050 Brussels, Belgium. [5]Department of Chemistry, Colby College, 4000 Mayflower Hill Drive, Waterville, Maine 04901.

ABSTRACT

Extant life relies on phospholipid membranes that selectively manage the flux of materials from one side to another. Prior to the development of such complex organic membranes, the separation of life from nonlife, or inside from outside, may have been achieved by geological inorganic barriers. Submarine alkaline hydrothermal vents, with their inherent pH gradients across inorganic mineral structures and a steady supply of H_2 and CO_2, are considered plausible environments for the transition from geochemistry to biochemistry. Analogous to extant life, which harnesses proton gradients for CO_2 reduction, these vents may have facilitated early carbon fixation through electrochemical processes mediated by Fe(Ni)S minerals. To investigate the potential bottlenecks in such prebiotic scenarios, we electrochemically characterized the electron and ion conductivity of synthetic FeS, Fe(Ni)S, and Green Rust under aqueous conditions mimicking a hydrothermal vent interface, using electrochemical impedance spectroscopy (EIS). Our results reveal that these minerals exhibit substantial electronic conductivity (1.5×10^{-2} - 3.6×10^{-2} S/cm) and moderate ionic conductivity (1.01×10^{-6} – 6.22×10^{-5} S/cm). Contemporary phospholipid membranes, by contrast, allow significant ion passage but are electrically insulating. These findings provide insights into the physicochemical properties of hydrothermal vent minerals and their potential role in facilitating early prebiotic reactions. Specifically, we introduce to the pH gradient hypothesis the concept of ion conductivity as a possible limiting factor on the flow of electrons needed for the production of organics across vent mineral barriers.

INTRODUCTION

What separates life from non-life? Philosophically, countless ideas have been proposed, including the ability to replicate, to metabolize, to grow and to die.[1, 2] A common feature of all known life is its physical organization into cellular systems compartmentalized by phospholipid membranes[3], which are thermo-oxidatively and electrochemically stable electrical insulators that are permeable to gasses[4, 5] and that selectively permit the flux of specific ions at specific times.[6]

Hadean submarine hydrothermal vents have long been proposed as potential hatcheries for life,[7-9] due to the presence of interfaces containing mineral that may have acted as metalloenzyme precursors, mediating key protometabolic reactions analogous to those occurring on cell membranes.[10-12] In such environments, protometabolic steps are hypothesized to have been driven by natural electrochemical gradients at these interfaces, potentially seeding the emergence of metabolism.[13, 14]

Drawing from clues in extant life, researchers have focused on early alkaline hydrothermal vents (AHVs). These vents likely hosted alkaline H_2-rich fluids that were separated from their surroundings by an inorganic barrier containing Fe(Ni)S mineral clusters and mixed-valence iron oxyhydroxides, also known as green rust (GR), such as fougerite.[15-18] Such barriers can also help sustain a pH gradient between the vent interior and the mildly acidic (pH 5.5), CO_2- and metal-rich early ocean.[19, 20 17, 21] This structural organization resembles (and may even be homologous to) the setting extant methanogens and acetogens utilize pH gradients, maintained by active proton pumping, to drive CO_2 reduction by H_2 oxidation. In methanogens, the pH gradient serves as an energetic driving for intracellular reduction reactions, which are catalyzed by various enzymes whose active sites contain Fe(Ni)S clusters. A hypothesis that has captured the interest of phylogeneticists and molecular biologists alike is the possibility that CO_2 reduction via H_2 oxidation in AHVs represents a geochemical analogue of the Wood–Ljungdahl Acetyl-CoA pathway, a metabolic pathway believed to date back to the last universal common ancestor (LUCA).[7, 22, 23] The fact that this is the only known CO_2 fixation pathway shared by both bacteria and archaea supports the idea that it may predate the divergence of these domains. It is therefore possible that the Wood–Ljungdahl pathway, or a simpler precursor, was used by LUCA or prevalent in prebiotic chemistry.

Several recent studies have demonstrated the feasibility of prebiotic scenarios in which pH gradients drive the coupling of CO_2 reduction and H_2 oxidation across Fe(Ni)S-containing inorganic barriers in hydrothermal systems.[19, 20, 24] To better understand the underlying mechanisms of these laboratory analogues, we must identify the factors driving or limiting this reaction. The electrical conductivity of individual crystals on the nanoscale has been raised as a possible bottleneck for CO_2 reduction, and the permeability of these barriers to different ions has been explored[25]. The kinetics of surface processes has also been considered as a possible limiting factor for reactivity.[26] We summarize in Figure 1 the four most likely processes that may act as bottlenecks: (a) electron conductivity (Figure 1a), ion transport (Figure 1b), the kinetics of CO_2 reduction (Figure 1c), and the kinetics of H_2 oxidation (Figure 1d).

In the present work, we focus on the conductivity of AHV inorganic barriers. On the macroscopic scale, electron and ion transport across barriers are intrinsically linked: to maintain charge balance, electron flow cannot outpace ion flow, and vice versa, despite the fact that the local transport mechanisms differ (electrons can move through conductive mineral structures, whereas ions pass through pores and channels). However, the extent to which either electron or ion transport limits the overall CO_2 reduction in prebiotic hydrothermal systems remains unclear. Consequently, a growing body of literature is focused on electrochemical characterization of hydrothermal vent minerals.[24–28] In this context, the purpose of this study is to determine the

electronic and ionic conductivities of synthetic hydrothermal vent minerals and to compare them to the electrical conductivities observed in extant life.

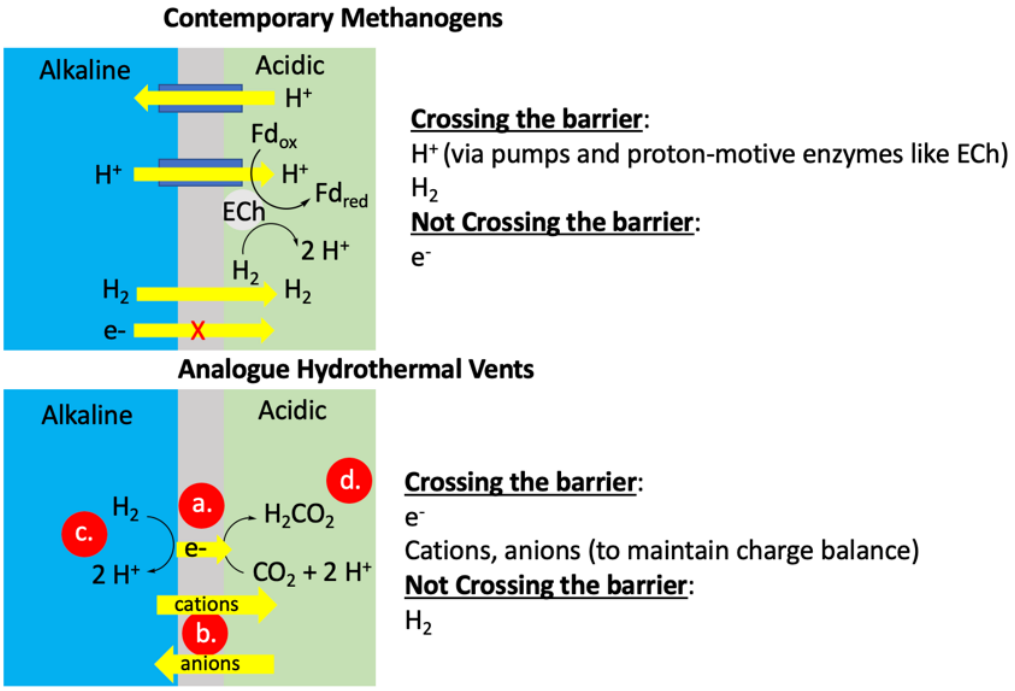

Figure 1. Ion, electron, and molecular passage across barriers in contemporary methanogens and hydrothermal vent minerals.

To investigate the conductivity properties of our synthetic vent minerals, we employed models based on electrochemical impedance spectroscopy (EIS) data. This technique uses small perturbations of a system under electrochemical equilibrium, and the relation between the impedance of a system and the frequency of that perturbation. From those relations, equivalent circuit models can be developed to extract parameters related to electron conductivity, ion transport and capacitive effects at the interface.

We used this approach to compare the modern chemiosmotic mechanism operating at biological membranes (Figure 1) with a proposed precursor to chemiosmosis. In the latter case, Fe(Ni)S minerals within an inorganic barrier are hypothesized to mediate catalytic CO_2 reduction driven by a pH gradient similar to that used in extant life - but through electrochemical rather than proton-motive mechanisms.

METHODS

Preparation of Minerals and Solutions

All solutions were prepared with high-purity water (Milli-Q system, 18.2 MΩ.cm) and reagent-grade chemicals. The electrolytes were prepared as previously described.[19, 24, 27] For gas saturation of solutions, N_2, CO_2 and H_2 (highly pressurized, purity: 99.99%) were used.

FeS and Fe(Ni)S samples were synthesized by co-precipitation: 50 mM $FeCl_2$ (and optionally 5 mM $NiCl_2$ for Fe(Ni)S) was reacted with 100 mM Na_2S as previously described.[8, 19, 24, 27] In this work, ocean analog and vent fluid analogs were mixed in a 1:1 ratio to form the precipitated synthetic Fe-S mineral.

Electrochemical Methods

Using a PTFE electrode jig as shown in Figure 2, experiments were performed using a two-electrode setup using an Admiral Squidstat Plus potentiostat. In the small channel between the two graphite electrodes, we placed wet mineral pastes. The geometric surface area of the electrode that was in contact with the electrolyte was 28.58 mm^2. Fe(Ni)S minerals were synthesized by the co-precipitation mentioned above. In addition, moisturized commercial mineral powders were also tested. For commercial samples, ~1 g of powder was mixed with 5 mL of ocean analog fluid, followed by centrifugation at 6000 rpm for 30 minutes. The resulting paste (for both synthetic and commercial samples) was transferred to the jig channel between the electrodes. A quartz cover slip was placed over the paste to seal the assembly. All mineral pastes were hydrated with ocean analog fluid to simulate conditions expected in early submarine hydrothermal systems.

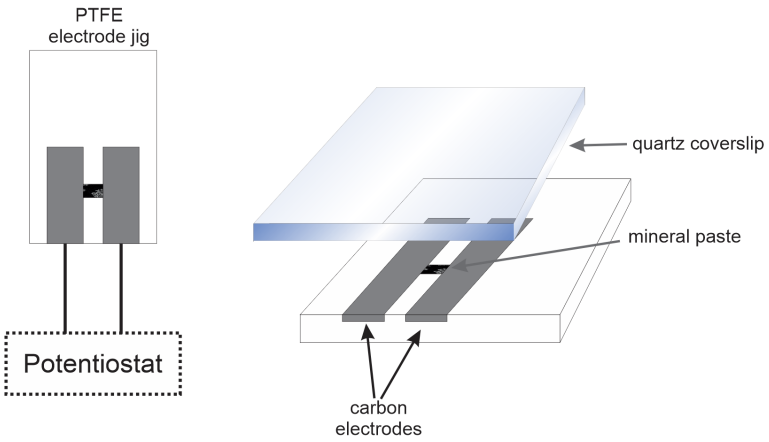

Figure 2. PTFE setup developed to investigate Fe-based mineral barrier properties under electrochemical conditions of the hydrothermal-vent interface.

Potentiostatic Electrochemical Impedance Spectroscopy (PEIS) was used to characterize the minerals in an electrochemical setting simulating an early hydrothermal vent interfaces. PEIS was performed at open circuit voltage (OCV) from 1 Hz to 1 MHz with an amplitude of 10 mV.

Calculation of Electrical and Ionic Conductivity

Electron conductivity values were obtained from the uncompensated resistance (R_u), determined from Nyquist plots or fitted from equivalent circuit models (see Table 1). Once resistance was known, resistivity (ρ) was calculated using equation (1), where L is the mineral

barrier thickness and A is the contact area. Conductivity was then obtained as the inverse of resistivity, as shown in equation (2).

$$\rho = \frac{R_u \times A}{L} \tag{1}$$

$$\sigma = \frac{1}{\rho} \tag{2}$$

Ionic conductivity was estimated based on the Warburg coefficient A_w obtained from the Warburg region in each EIS spectrum's Nyquist plot. This coefficient is related to the diffusion of dissolved species by equation (3),

$$A_w = \frac{4\,R\,T}{\sqrt{2}\,n^2\,F^2 A\,C} \times \frac{1}{\sqrt{D}}\ , \tag{3}$$

where R is the gas constant and F is the Faraday constant, T is absolute temperature, n is the charge transfer number, A is the electrode contact area, C is the concentration of dissolved ion and D is the diffusion coefficient. The ion equivalent conductivity Λ was then calculated with equation (4):

$$\Lambda = z_i\ e_0\ F\ u_{abs}\ . \tag{4}$$

Here, z_i is the ion's formal charge, e_0 is the elementary charge (1.602×10^{-19} C), and u_{abs} the absolute mobility, calculated as $u_{abs} = D/kT$, with k being the Boltzmann constant.

RESULTS

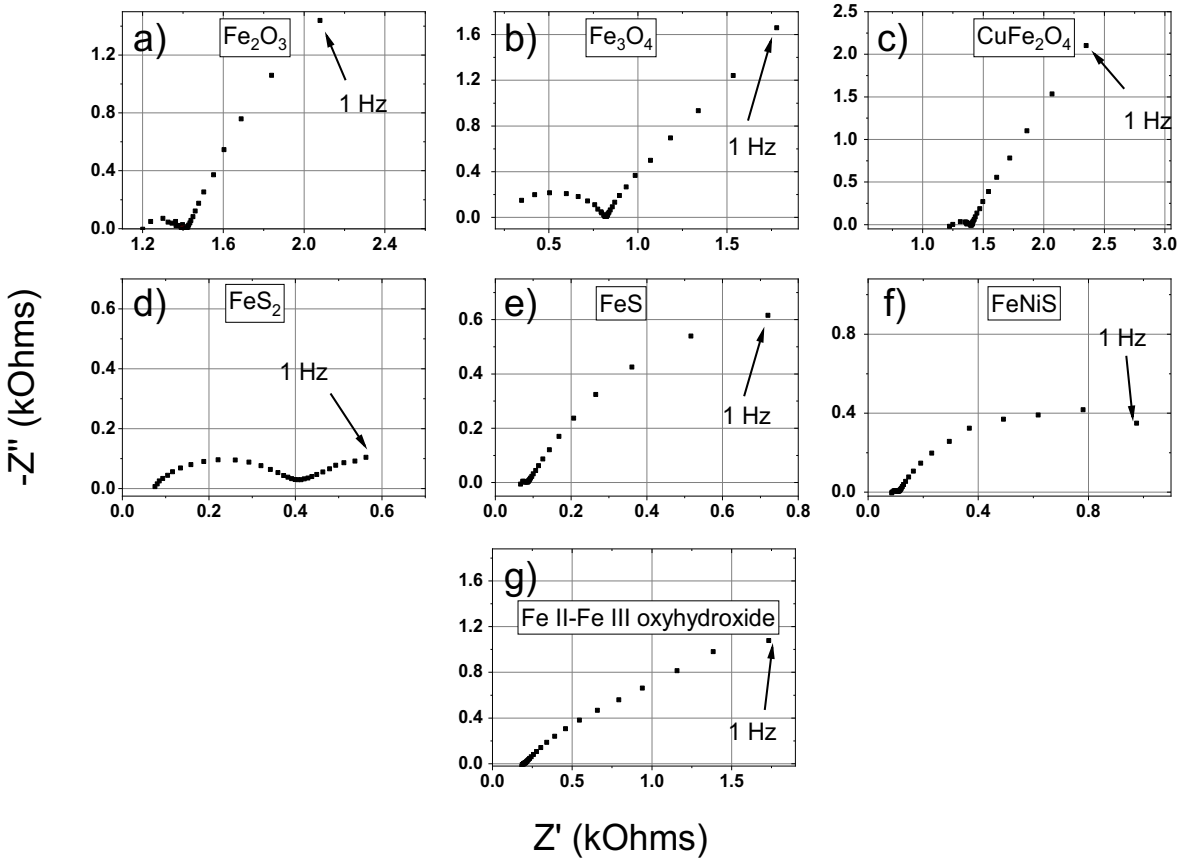

Figure 3. Nyquist plots from electrochemical impedance spectroscopy (EIS) results for different Fe-based minerals using our PTFE reactor setup.

Nyquist plots (Figure 3) are commonly used in the field of electrochemistry to represent EIS results. This plot displays Z' and -Z'' that represent, respectively, the imaginary and the real part of the impedance vector ($\mathbf{Z}(\omega)=Z'-jZ''$) in the complex plane, for different values of perturbation frequency. The plots shown in Figure 3 provided insight into the electronic and ionic conductivities of the mineral barriers under simulated hydrothermal vent electrochemical conditions. Focusing on FeS, FeNiS and green rust (GR), we fitted equivalent circuit models to their impedance data (Figure 4). These models were adapted from the work of Arzola and Genesca[28], which also guided our interpretation of each circuit element in terms of interfacial properties.[28] The models include components representing the double-layer capacitance (C_{dl}), the mineral film capacitance and resistance (C_{film} and R_{film} respectively), and the charge transfer resistance (R_{ct}). These parameters were extracted from fitting and are summarized in Table 1, along with the calculated electrical and ionic conductivities of each mineral.

As expected, FeS and green rust GR exhibited notable electrical conductivity, in accordance with previous works.[24, 29] The measured electronic conductivities (of the order of 10^{-2} S/cm) are comparable to those of some semiconductors, conductive polymers and saline solutions. These materials also demonstrated moderate ionic conductivity, likely facilitated by the disordered nature of the hydrated mineral paste, allowing for ion movement through the aqueous phase between mineral grains.

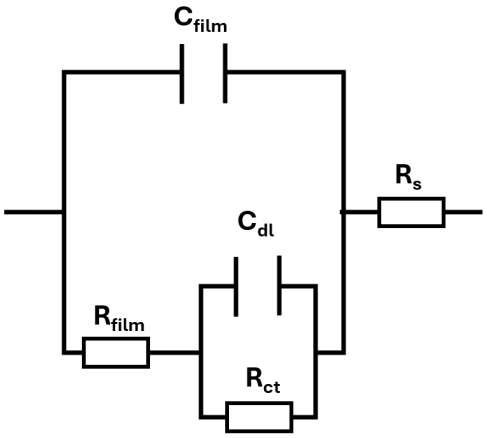

Figure 4. Equivalent circuit model for the fitting of experimental data for FeS, FeNiS and Green rust minerals EIS. Each circuit is a model for the double layer capacitance (C_{dl}), mineral film capacitance and resistance (C_{film} and R_{film} respectively), or the charge transfer resistance (R_{ct}).

Table 1. Component values of the equivalent circuit shown in Figure 3 for the EIS data fitting and calculated electrical and ionic conductivities of different synthetic Fe-based minerals under hydrothermal-vent conditions.

Mineral	R_s (Ohm)	R_{ct} (Ohm)	C_{dl} (μF)	R_{film} (Ohm)	C_{film} (μF)	Conductivity (S/cm)	
						electrical	ion
FeS	84.1	1003.9	89.9	256.3	52.9	3.6×10^{-2}	6.22×10^{-5}
Fe(Ni)S	106.6	341.4	118.7	799.8	31.9	2.8×10^{-2}	2.96×10^{-6}
Green Rust	194.5	1×10^{6}	487.33	4486.4	123.79	1.5×10^{-2}	1.01×10^{-6}

DISCUSSION

Modern cells tightly regulate ion transport across membranes using active and passive mechanisms, yet their membranes are essentially insulating to electrons (electrical conductivity ≈ 5×10^{-10} S·cm^{-1})[21]. In contrast, the Fe-based minerals we investigated have significantly higher electrical conductivities (1.5×10^{-2} - 3.6×10^{-2} S·cm^{-1}) and only moderate ion conductivities (1.01×10^{-6} – 6.22×10^{-5} S·cm^{-1}).

Contemporary methanogens create and exploit proton gradients across their membranes by actively pumping H^+ ions out of the cell. The return of protons down this gradient powers energy-requiring reactions such as ferredoxin reduction via hydrogen oxidation, catalyzed by the membrane-bound proton-motive enzyme Ech. In this process, H^+ and H_2 can permeate the membrane, but electrons cannot. Prior studies of hydrothermal vent analogs[22] suggest that the reducing species crossing mineral barriers may not be H_2, but rather free electrons. However, if electrons do traverse the barrier, maintaining charge neutrality would require a counter-balancing ionic flux, via either co-moving cations, oppositely moving anions, or a combination of both. Our findings suggest that while mineral barriers allow efficient electron transfer, ion transport is

considerably more limited. Thus, under prebiotic conditions, the rate of ion flux required to maintain electroneutrality may represent a bottleneck for sustained protometabolic activity and the formation of organic products.

CONCLUSIONS

Our electrochemical characterization of synthetic FeS, Fe(Ni)S, and green rust under simulated hydrothermal vent conditions revealed that these minerals exhibit significant conductivity for electrons and moderate conductivity for ions. These properties support the hypothesis that such mineral barriers could mediate electron transport across redox and pH gradients in early Earth environments, facilitating prebiotic CO_2 reduction coupled to H_2 oxidation. Our results suggest that electron transport is unlikely to be the limiting step for protometabolic redox reactions at mineral interfaces. Instead, the comparatively slower ion transport may impose constraints on the rate or extent of organic synthesis. These findings offer quantitative insight into the electrochemical behavior of Fe-based minerals, and their relevance to scenarios of early prebiotic chemistry relying on the electrochemical coupling of H_2 oxidation on one side of a mineral barrier with the reduction of organics on the other side.

References

1. Margulis, L.; Sagan, D., *What is life?* Univ of California Press: 2000.
2. Benner, S. A., Defining life. *Astrobiology* **2010,** *10* (10), 1021-1030.
3. Lombard, J.; López-García, P.; Moreira, D., The early evolution of lipid membranes and the three domains of life. *Nat. Rev. Microbiol.* **2012,** *10* (7), 507-515.
4. Itel, F.; Al-Samir, S.; Öberg, F.; Chami, M.; Kumar, M.; Supuran, C. T.; Deen, P. M.; Meier, W.; Hedfalk, K.; Gros, G., CO2 permeability of cell membranes is regulated by membrane cholesterol and protein gas channels. *The FASEB Journal* **2012,** *26* (12), 5182-5191.
5. Subczynski, W. K.; Hyde, J. S.; Kusumi, A., Oxygen permeability of phosphatidylcholine--cholesterol membranes. *Proc. Natl. Acad. Sci.* **1989,** *86* (12), 4474-4478.
6. Hauser, H.; Phillips, M.; Stubbs, M., Ion permeability of phospholipid bilayers. *Nature* **1972,** *239* (5371), 342-344.
7. Martin, W.; Baross, J.; Kelley, D.; Russell, M. J., Hydrothermal vents and the origin of life. *Nat. Rev. Microbiol.* **2008,** *6* (11), 805-814.
8. Sojo, V.; Herschy, B.; Whicher, A.; Camprubi, E.; Lane, N., The origin of life in alkaline hydrothermal vents. *Astrobiology* **2016,** *16* (2), 181-197.
9. Martin, W.; Russell, M. J., On the origin of biochemistry at an alkaline hydrothermal vent. *Philos. Trans. R. Soc. B* **2007,** *362* (1486), 1887-1926.
10. Altair, T.; Borges, L. G.; Galante, D.; Varela, H., Experimental approaches for testing the hypothesis of the emergence of life at submarine alkaline vents. *Life* **2021,** *11* (8), 777.
11. Lane, N., Proton gradients at the origin of life. *BioEssays* **2017,** *39* (6), 1600217.
12. Nitschke, W.; Farr, O.; Gaudu, N.; Truong, C.; Guyot, F.; Russell, M. J.; Duval, S., The winding road from origin to emergence (of life). *Life* **2024,** *14* (5), 607.

13. Russell, M. J.; Nitschke, W.; Branscomb, E., The inevitable journey to being. *Philos. Trans. R. Soc. B, Biol. Sci.* **2013,** *368* (1622), 20120254.
14. Yamaguchi, A.; Li, Y.; Takashima, T.; Hashimoto, K.; Nakamura, R., CO 2 reduction using an electrochemical approach from chemical, biological, and geological aspects in the ancient and modern Earth. *Solar to Chemical Energy Conversion: Theory and Application* **2016**, 213-228.
15. Génin, J.-M.; Renard, A.; Ruby, C., Fougerite FeII− III oxyhydroxycarbonate in environmental chemistry and nitrate reduction. *Hyperfine Interactions* **2008,** *186* (1), 31-37.
16. Duval, S.; Baymann, F.; Schoepp-Cothenet, B.; Trolard, F.; Bourrié, G.; Grauby, O.; Branscomb, E.; Russell, M. J.; Nitschke, W., Fougerite: The not so simple progenitor of the first cells. *Interface Focus* **2019,** *9* (6), 20190063.
17. Herschy, B.; Whicher, A.; Camprubi, E.; Watson, C.; Dartnell, L.; Ward, J.; Evans, J. R.; Lane, N., An origin-of-life reactor to simulate alkaline hydrothermal vents. *J. Mol. Evol.* **2014,** *79* (5-6), 213-227.
18. Russell, M. J.; Ponce, A., Six 'must-have'minerals for life's emergence: Olivine, pyrrhotite, bridgmanite, serpentine, fougerite and mackinawite. *Life* **2020,** *10* (11), 291.
19. Hudson, R.; de Graaf, R.; Rodin, M. S.; Ohno, A.; Lane, N.; McGlynn, S. E.; Yamada, Y. M.; Nakamura, R.; Barge, L. M.; Braun, D., CO2 reduction driven by a pH gradient. *Proc. Natl. Acad. Sci.* **2020,** *117* (37), 22873-22879.
20. Barge, L. M.; Flores, E.; Baum, M. M.; VanderVelde, D. G.; Russell, M. J., Redox and pH gradients drive amino acid synthesis in iron oxyhydroxide mineral systems. *Proc. Natl. Acad. Sci.* **2019,** *116* (11), 4828-4833.
21. Ooka, H.; McGlynn, S. E.; Nakamura, R., Electrochemistry at deep-sea hydrothermal vents: utilization of the thermodynamic driving force towards the autotrophic origin of life. *ChemElectroChem* **2019,** *6* (5), 1316-1323.
22. Martin, W. F.; Sousa, F. L.; Lane, N., Energy at life's origin. *science* **2014,** *344* (6188), 1092-1093.
23. Russell, M. J.; Martin, W., The rocky roots of the acetyl-CoA pathway. *Trends in biochemical sciences* **2004,** *29* (7), 358-363.
24. Altair, T.; Dragoti, E.-S.; Sojo, V.; Li, Y.; McGlynn, S.; Galante, D.; Varela, H.; Hudson, R., Carbon reduction powered by natural electrochemical gradients under submarine hydrothermal vent conditions. **2024**.
25. Vasiliadou, R.; Dimov, N.; Szita, N.; Jordan, S. F.; Lane, N., Possible mechanisms of CO2 reduction by H2 via prebiotic vectorial electrochemistry. *Interface Focus* **2019,** *9* (6), 20190073.
26. Živković, A.; Somers, M.; Camprubi, E.; King, H. E.; Wolthers, M.; de Leeuw, N. H., Changes in CO2 adsorption affinity related to Ni doping in FeS surfaces: A DFT-D3 study. *Catalysts* **2021,** *11* (4), 486.
27. Sojo, V.; Ohno, A.; McGlynn, S. E.; Yamada, Y.; Nakamura, R., Microfluidic reactors for carbon fixation under ambient-pressure alkaline-hydrothermal-vent conditions. *Life* **2019,** *9* (1), 16.
28. Arzola, S.; Genesca, J., The effect of H 2 S concentration on the corrosion behavior of API 5L X-70 steel. *Journal of Solid State Electrochemistry* **2005,** *9*, 197-200.
29. Purvis, G.; Šiller, L.; Crosskey, A.; Vincent, J.; Wills, C.; Sheriff, J.; Xavier, C.; Telling, J., Generation of long-chain fatty acids by hydrogen-driven bicarbonate reduction in ancient alkaline hydrothermal vents. *Communications Earth & Environment* **2024,** *5* (1), 30.